JOURNAL OF GEOPHYSICAL RESEARCH, VOL. 92, NO. A4, PAGES 3195–3206, APRIL 1, 1987

Simulation of Kelvin-Helmholtz Instability at the Magnetospheric Boundary

AKIRA MIURA

Geophysics Research Laboratory, University of Tokyo, Japan

A two-dimensional magnetohydrodynamic simulation of Kelvin-Helmholtz instability at the terrestrial magnetospheric boundary is performed by including gradients of plasma and magnetic field normal to the dayside low-latitude magnetospheric boundary. A magnetopause current layer is corrugated highly nonlinearly by the instability, and a plasma blob is formed by an interchange motion associated with the instability. The magnetosheath plasma flow momentum is diffused into the magnetosphere by the anomalous tangential (Reynolds plus Maxwell) stresses associated with the instability, and a wide velocity boundary layer is formed just inside the magnetopause current layer, while the thickness of the magnetopause current layer remains almost constant during the evolution of the instability. The convection voltage drop (integral of the convection electric field) across the velocity shear layer is amplified several times by the anomalous momentum transport associated with the instability. The anomalous momentum flux into the magnetosphere (tangential stress) reaches 0.6 to a few percent of the magnetosheath flow momentum flux, and this anomalous momentum flux into the magnetosphere is sufficient for accounting for the observed tailward momentum flux in the low-latitude boundary layer. The value of the anomalous viscosity ν_{ano} depends importantly on the magnetosheath Alfvén Mach number M_A, which is defined by a magnetosheath magnetic field component parallel to the magnetosheath flow velocity; for $M_A = 2.5$, ν_{ano} is equal to $\sim 0.014 \times 2aV_0$, where $2a$ is the thickness of the initial velocity shear layer and V_0 is the total jump of the flow velocity across the magnetospheric boundary, and it increases with M_A, and for $M_A > 5.0$ it is equal to $\sim 0.2 \times 2aV_0$. For a reasonable set of parameters at the dayside magnetospheric boundary the anomalous viscosity obtained is just the right magnitude for driving a magnetospheric convection in the terrestrial magnetosphere.

1. INTRODUCTION

Kelvin-Helmholtz (K-H) instability has long been studied regarding the stability of the magnetopause boundary between the solar wind plasma flow and the terrestrial magnetospheric plasma (e.g., *Dungey* [1955] and *Parker* [1958]; see also *Gerwin* [1968] and *Southwood* [1979]), and its importance in the "viscouslike interaction" at the terrestrial magnetopause boundary has recently been emphasized [*Miura*, 1982, 1984, 1985*b*]: *Axford and Hines* [1961] have suggested that a viscouslike interaction along the flanks of the magnetosphere can permit solar wind momentum to diffuse onto closed magnetospheric field lines. The resulting tailward convection flow would eventually be closed by an earthward return flow in the center of the tail, and a magnetospheric plasma convection (circulation) is formed inside the magnetosphere.

Since the magnetospheric plasma convection is a plasma circulation by $\mathbf{E} \times \mathbf{B}$ electric field drift, a good measure of the global plasma circulation is a total convection voltage drop (not necessarily electrostatic potential difference but an integral of the convection electric field) over the polar cap of the magnetosphere: The maximum of the convection voltage drop over the polar cap is 60–150 kV [*Reiff et al.*, 1981; *Wygant et al.*, 1983; *Doyle and Burke*, 1983], and its dominant component, which is controlled by a north-south component of the interplanetary magnetic field, is thought to be due to interconnection of interplanetary magnetic field lines with terrestrial magnetospheric field lines by dayside reconnection process [*Dungey*, 1961; *Petschek*, 1964; *Levy et al.*, 1964]; for detail of the reconnection process, see Vasyliunas [1975] and Sonnerup [1979], and for its importance in the magnetospheric convection, see Cowley [1982]. An important and quite interesting observation of the plasma convection inside the terrestrial magnetosphere, however, is that this plasma circulation inside the magnetosphere has a residual component which is not controlled by the north-south component of the interplanetary magnetic field [*Reiff et al.*, 1981; *Wygant et al.*, 1983; *Doyle and Burke*, 1983]. According to suggestions by *Axford and Hines* [1961], it is natural to hypothesize that this observed residual plasma convection is caused by some viscouslike interaction between the flowing magnetosheath plasma and the stationary magnetospheric plasma. Although such a viscouslike contribution to the magnetospheric convection appears to be small (5–30 kV) in comparison with a reconnection-induced convection voltage drop, the determination of the physical mechanism of the "viscouslike interaction" and its contribution to the magnetospheric convection by its tangential stress is important for complete understanding of the solar wind–magnetosphere interaction.

In pursuing a viscouslike interaction process at the terrestrial magnetopause boundary we must notice that a classical viscosity by ion-ion Coulomb collision is negligibly small to explain the tangential stress necessary for the observed residual plasma convection; the viscosity at the magnetopause boundary must therefore be essentially "anomalous," and some anomalous plasma process must be responsible for yielding the required momentum transport or the required viscosity. Although there is no present agreement as to the exact physical mechanism involved in the viscouslike drag at the magnetopause, it has been demonstrated [*Miura*, 1982, 1984, 1985*b*] by using a magnetohydrodynamic (MHD) simulation that the Kelvin-Helmholtz instability gives an anomalous viscosity necessary for the "viscouslike interaction" at the magnetopause. In that simulation it is demonstrated that when the magnetosheath flow velocity (or the total velocity jump at the magnetopause) is super-Alfvénic with respect to a magnetic

Paper number 6A8610.
0148-0227/87/006A-8610$05.00

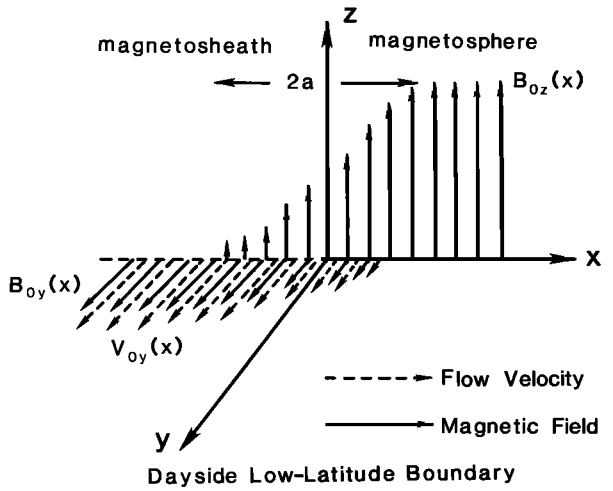

Fig. 1. A model of the finite thick tangential discontinuity representing the dayside low-latitude magnetospheric boundary on the equatorial plane.

field component parallel to the flow velocity, the shear flow at the magnetopause becomes unstable to the Kelvin-Helmholtz instability and gives rise to a viscouslike drag by finite Reynolds and Maxwell stresses by the instability. Since the magnetosheath Alfvén Mach number M_A, which is defined by a magnetosheath magnetic field component parallel to the magnetosheath flow velocity is a variable depending on the interplanetary magnetic field and on the external flow (magnetosheath flow), it is important to see how the K-H viscouslike interaction, that is, the anomalous momentum transport by the K-H instability, is controlled by the external condition (magnetosheath Alfvén Mach number M_A). The purpose of this paper is therefore to extend further the previous simulation model [*Miura*, 1985*b*] including gradients of plasma and magnetic field normal to the magnetopause and to investigate the dependence of the Kelvin-Helmholtz instability on the external variable (magnetosheath Alfvén Mach number M_A) and thus to obtain a more complete understanding of the K-H viscouslike interaction at the terrestrial magnetospheric boundary.

In section 2 we explain a model of the dayside low-latitude magnetospheric boundary. Numerical results are presented and discussed in section 3. Section 4 contains a summary of results and discussion of their implications in the viscouslike interaction at the terrestrial magnetospheric boundary.

2. MODEL

In the present simulation we assume that a magnetospheric boundary is a "finite thick tangential discontinuity" because the magnetopause current layer and the velocity shear layer at the boundary are at least several finite Larmor radii thick [e.g., *Parker*, 1967; *Berchem and Russell*, 1982]; such a tangential discontinuity is at times observed on the dayside magnetospheric boundary [*Papamastorakis et al.*, 1984]. It is also known that an initial value treatment of the Kelvin-Helmholtz instability is improperly posed for the velocity shear layer of zero thickness [*Richtmyer and Morton*, 1967].

Shown in Figure 1 is an MHD model of the finite thick tangential discontinuity representing the dayside low-latitude magnetospheric boundary on the equatorial plane (although we are aware that the use of MHD at the magnetopause is in a sense doubtful, for example, finite Larmor radius effect, anisotropic pressure effect, we believe that an MHD approach is a necessary first step toward complete understanding of the magnetopause stability). In this model the magnetospheric boundary, where two different plasmas are in contact, is characterized by the shear in the flow velocity, the change of the magnetic field, and the gradient of the plasma density: The magnetosheath plasma is flowing with a velocity V_0, and the magnetospheric plasma is stationary with a transition represented by a hyperbolic tangent velocity shear profile. The magnetosheath magnetic field (solid arrows) is taken parallel to the flow (dashed arrows), and the magnetospheric magnetic field is taken transverse to the magnetosheath flow. In this MHD model of the finite thick tangential discontinuity the ratio of the thickness of the velocity shear layer to the magnetopause thickness is arbitrary, but for simplicity we assume in the present model that this ratio is equal to unity. Therefore in order to represent that both flow velocity and magnetic field are changed in the same thickness $2a$ we express the flow velocity $v_{0y}(x)$ and y and z components of the magnetic field as follows:

$$v_{0y}(x) = (V_0/2)[1 - \tan h(x/a)] \quad (1)$$

$$B_{0y}(x) = (B_0/2)[1 - \tan h(x/a)] \quad (2)$$

$$B_{0z}(x) = (B_0/2)[(1+\beta_{SH})/(1+\beta_{SP})]^{1/2}[1+\tan h(x/a)] \quad (3)$$

where β_{SH} and β_{SP} are the plasma $\beta(\beta = 2\mu_0 p_0/B_0^2)$ in the magnetosheath and in the magnetosphere, respectively. The plasma pressure is taken to satisfy the total pressure balance. The plasma temperature is assumed uniform across the boundary. The magnetosheath flow is characterized by the

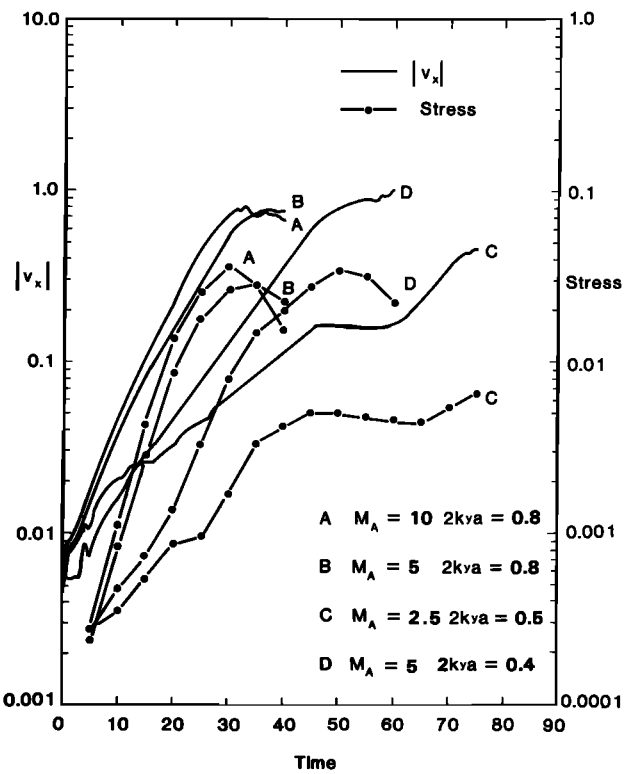

Fig. 2. Temporal evolution of the peak of the x component of the flow velocity $|v_x|$ normalized by V_0 (solid lines) and the peak of the spatial average over one wave period of the total stress normalized by $\rho_0 V_0^2$ (dot-dash lines) for different periodicity lengths L_y and for different Alfvén Mach numbers M_A in the magnetosheath.

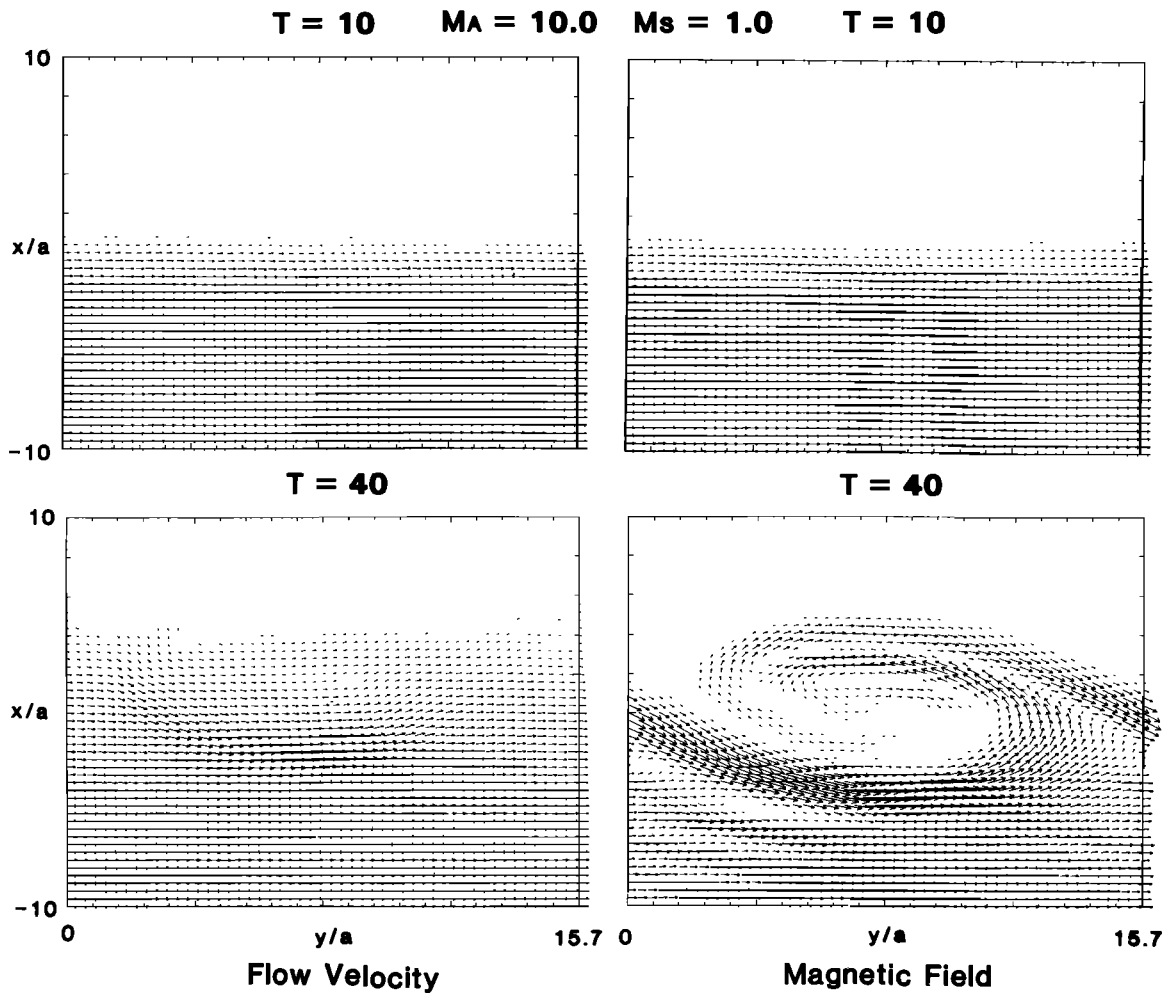

Fig. 3. Flow velocity vectors (left panels) and magnetic field vectors (right panels) at initial ($T = 10$) and quasi-stationary ($T = 40$) stages for the case of $M_A = 10$, $M_S = 1.0$, and $2k_y a = 0.8$ (case A of Figure 2).

Alfvén Mach number $M_A = V_0/v_A$, and the sound Mach number $M_S = V_0/c_S$, where v_A and c_S are the Alfvén speed and the sound speed in the magnetosheath, respectively. The plasma β in the magnetosheath is given by $(3/2)(M_A/M_S)^2$ and that in the magnetosphere β_{SP} is 0.2. A periodic boundary condition is imposed at $y = 0$ and $y = L_y$. In the x direction we have placed boundaries at $x = \pm 10a$, which are far enough from the velocity shear region to make boundary effects negligible. Two-step Lax-Wendroff method [*Richtmyer and Morton*, 1967] with an artificial viscosity term [*Lapidus*, 1967] is used to solve MHD equations. Time is normalized by $2a/V_0$. More detail regarding the numerics used is described by *Miura* [1985*a*].

3. Numerical Results

MHD simulation is initiated by adding a small seed of unstable perturbation to the flowing equilibrium described by equations (1)–(3). The small seed of unstable perturbation has a peak velocity v_x equal to $0.005V_0$ and a wavelength equal to L_y, and hence the K-H instability is treated as an absolute instability in the present simulation.

Figure 2 shows temporal evolution of the peak of the x component of the flow velocity $|v_x|$ normalized by V_0 (solid lines) and peak of the spatial average over one wave period of the total (Reynolds plus Maxwell) stress $-\langle \rho v_x v_y - \mu_0^{-1} B_x B_y \rangle$ normalized by $\rho_0 V_0^2$ (dot-dash lines), where the angular bracket represents the spatial average over one wave period and ρ_0 is the plasma density in the magnetosheath, for different periodicity lengths L_y and for different Alfvén Mach numbers M_A in the magnetosheath. For all cases treated in the present study, sound Mach number M_S in the magnetosheath is 1.0. Using the wave number k_y of an unstable mode, the periodicity length L_y is given by

$$L_y = 2\pi/k_y \tag{4}$$

For $M_A = 5.0$ and $M_S = 1.0$ the wave number satisfying $2k_y a = 0.8$ is nearly equal to the wave number of the fastest growing unstable mode. Figure 2 shows that after initial irregular evolutions of the velocity perturbations owing to the difference between the initial seed of the unstable perturbation and the exact unstable eigenfunction, all cases show linear growths of the velocity perturbations $|v_x|$, which tend to saturate in a later period. It should be emphasized here that the case of longer wavelength $M_A = 5$ and $2k_y a = 0.4$ (case D) has smaller growth rate than the case of $M_A = 5$ and $2k_y a = 0.8$ (case B) but has a slightly larger saturation amplitude than the case of $2k_y a = 0.8$ (case B); it seems therefore that the longer-wavelength mode has a larger saturation amplitude than the shorter-wavelength mode. Such a tendency has already been noted in a simulation of the electrostatic transverse K-H insta-

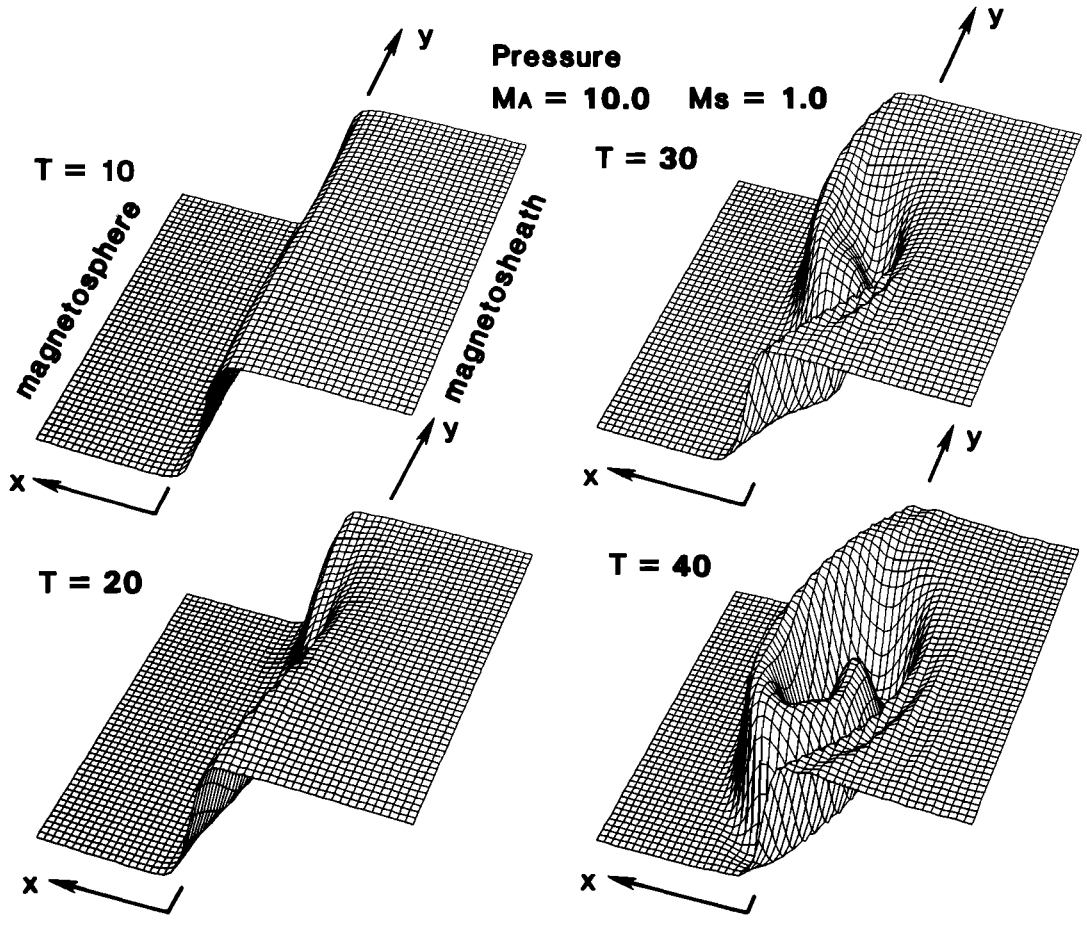

Fig. 4. Three-dimensional views of the plasma pressure at four different times for $M_A = 10$, $M_S = 1.0$, and $2k_y a = 0.8$ (case A of Figure 2).

bility [*Pritchett and Coroniti*, 1984]; they have found that in a later period of the evolution of the electrostatic transverse K-H instability a long-wavelength mode dominates plasma dynamics. For cases A, B, and D the total stress reaches 2–4 $\times 0.01\rho_0 V_0^2$; this means that about 2–4% of the flow momentum flux in the magnetosheath is transported into the magnetosphere by the K-H instability. The case A of $M_A = 10$ and $2k_y a = 0.8$ has the largest growth rate, since the stabilizing tension force of the magnetic field lines in the magnetosheath is smallest and reaches a slightly larger amplitude than the case of $M_A = 5$ and $2k_y a = 0.8$ (case B). Owing to a large stabilizing tension force of magnetic field lines, the case C of Figure 2 ($M_A = 2.5$ and $2k_y a = 0.5$) has the smallest growth rate, and the total stress for this case reaches $0.006\rho_0 V_0^2$.

Figure 3 shows flow velocity vectors (left panels) and magnetic field vectors (right panels) at initial ($T = 10$) and quasi-stationary ($T = 40$) stages for the case of $M_A = 10$, $M_S = 1.0$, and $2k_y a = 0.8$ (case A of Figure 2). The parallel shear flow in the initial stage (top left panel) is disturbed very strongly at $T = 40$; by this time the gradient of the flow velocity has been diffused quite markedly (bottom left panel), and a large flow in the positive y direction is induced in the region $x > 0$, which was originally the stationary magnetosphere. This formation of a wide velocity shear layer from an initially narrow velocity shear layer is due to the anomalous momentum transport associated with the K-H instability. In addition to the relaxation of the flow velocity shear and a consequent diffusion of the flow velocity from the magnetosheath into the magnetosphere it is seen in the bottom left panel that the plasma flow is accelerated slightly where the initial straight flow is deflected most by the vortex motion. Such a flow acceleration by the K-H instability has already been noted for the K-H instability in a uniform plasma [*Miura*, 1984], and it occurs because the flow vortex motion is added onto the undisturbed background flow. As we shall see later, this flow acceleration occurs in coincidence with the increase of the x component of the electric field E_x and thus the accelerated flow is mainly due to the increase of the $\mathbf{E} \times \mathbf{B}$ motion of the plasma. Right panels show that the magnetopause current layer (a region of the magnetic field gradient) also undulates with time and at $T = 40$ the magnetic field lines in the magnetosheath are stretched and twisted and the magnetopause current layer is corrugated highly nonlinearly (bottom right panel). In contrast to the flow evolution shown in the left panels the magnetopause current layer characterized by a steep gradient of the magnetic field has still a clear field gradient at $T = 40$. This is because in the present ideal MHD with frozen-in constraint the K-H instability gives an anomalous viscosity but not an anomalous resistivity, which is necessary to diffuse the magnetopause current layer.

Figure 4 shows three-dimensional views of the plasma pressure at four different times for $M_A = 10$, $M_S = 1.0$, and $2k_y a = 0.8$ (case A of Figure 2). The initially straight mag-

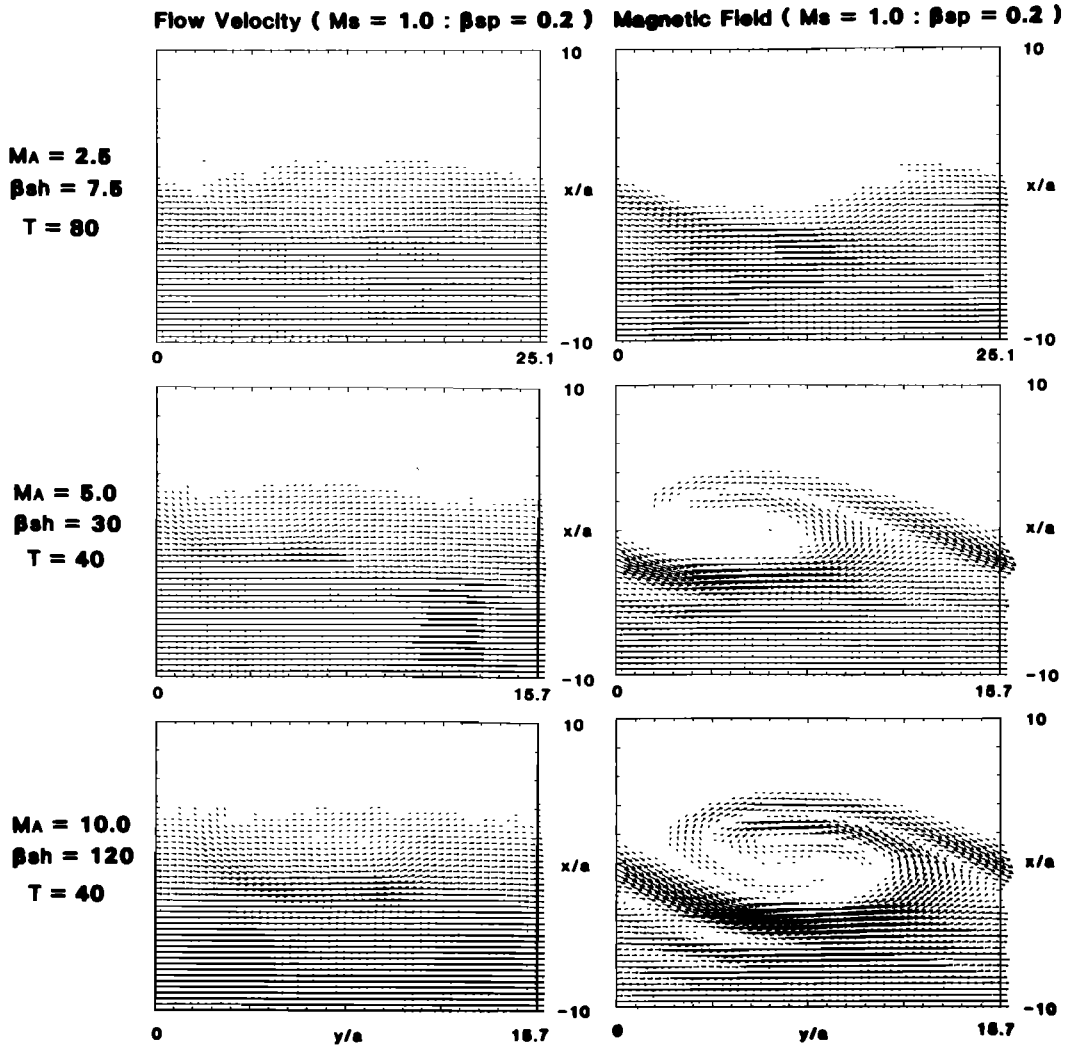

Fig. 5. Flow velocity vectors (left panels) and magnetic field vectors (right panels) at quasi-stationary stages for three different values of M_A (cases A, B, and C of Figure 2).

netopause boundary (characterized by steep pressure gradient) is undulated with time, and at $T = 40$ the magnetopause boundary is deformed in a very complicated, highly nonlinear manner to form a plasma blob in $x > 0$ as a result of the interchange motion by the K-H instability. These panels demonstrate clearly how the plasma of the high-pressure side (magnetosheath) tends to penetrate into the low-pressure side (magnetosphere) owing to the interchange motion associated with the K-H instability. Notice, however, that owing to the frozen-in constraint in the ideal MHD, the transport of magnetosheath plasma through the magnetopause onto closed field lines of the magnetosphere is inhibited and the plasma blob formed in $x > 0$ is still threaded by magnetic field lines of the magnetosheath; namely, although the momentum and energy are transported across the magnetopause to form a velocity boundary layer within the magnetopause by the present MHD process, the plasma mass can not be transported across the magnetopause by the present ideal MHD process.

Figure 5 shows flow velocity vectors (left panels) and magnetic field vectors (right panels) at quasi-stationary stages for three different M_A (cases A, B, and C of Figure 2). As M_A increases, the stabilizing tension force of magnetic field lines decreases in the magnetosheath, and the growth rate of the instability increases (see Figure 2). For all three cases, left panels show that the initial flow velocity gradients are diffused quite markedly by the instability in the quasi-stationary stages. Right panels show that for $M_A = 5$ and 10 (cases B and A of Figure 2) the magnetopause boundary characterized by large gradient of the magnetic field is corrugated highly nonlinearly and this corrugation of the magnetopause boundary is more noticeable for larger M_A. It is also seen in right panels that the magnetic field is amplified along the magnetopause by converging flows.

Figure 6 shows three-dimensional views of top surfaces of the plasma pressure distribution in the quasi-stationary stages for the same three cases as shown in Figure 5. For $M_A = 2.5$ (case C of Figure 2) the corrugation of the magnetopause boundary characterized by the large pressure gradient is small, but for $M_A = 5$ and 10 the magnetopause boundaries are corrugated highly nonlinearly by the interchange motion associated with the K-H instability. These panels demonstrate clearly how the plasma in the magnetosheath tends to penetrate

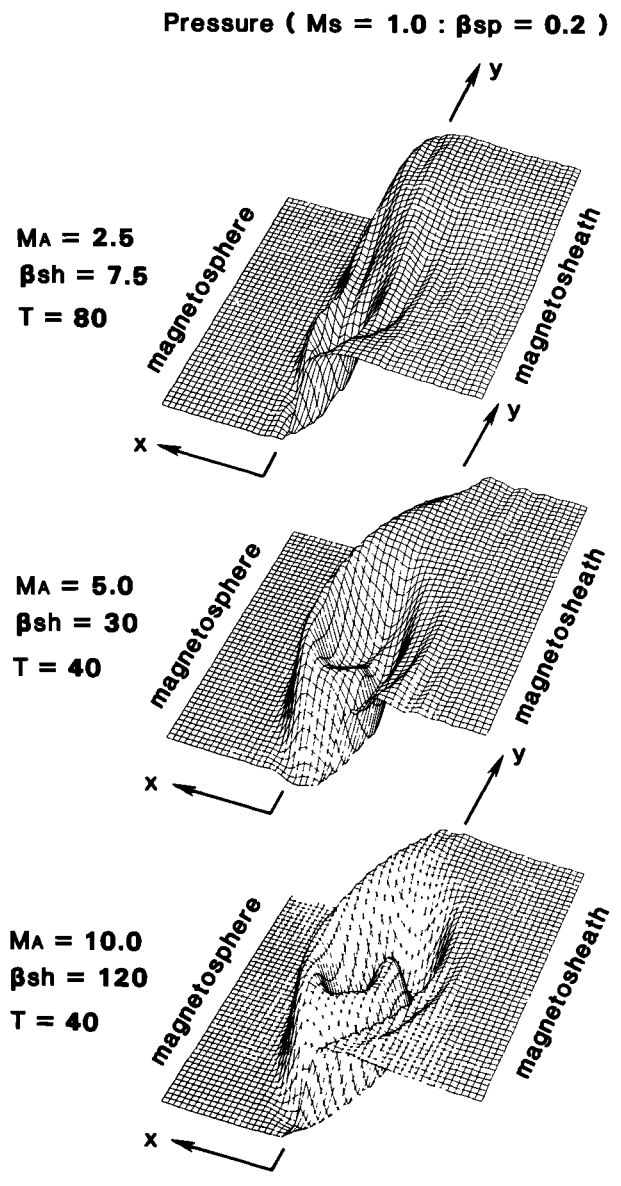

Fig. 6. Three-dimensional views of top surfaces of the plasma pressure distribution in the quasi-stationary stages for the same three cases as shown in Figure 5.

into the magnetosphere by the K-H instability; this tendency is larger for larger Alfvén Mach number M_A or for larger plasma β in the magnetosheath.

In order to see effects of changing the wavelength (periodicity length) on the development of the K-H instability we show in Figure 7 flow velocity vectors (top left), magnetic field vectors (bottom left), and a three-dimensional view of top surface of the plasma pressure (right) at $T = 60$ for $2k_y a = 0.4$, $M_A = 5.0$, and $M_S = 1.0$ (case D of Figure 2). It is obvious that this case with longer wavelength has much wider perturbation in the x direction than the middle panels of Figure 5 and 6 for $2k_y a = 0.8$. In comparison with the case of $2k_y a = 0.8$ (see middle panels of Figures 5 and 6) this case with longer wavelength shows larger flow acceleration (top left panel) than the case of $2k_y a = 0.8$ (see middle panels of Figure 5).

Figure 8 shows profiles (cross sections) as a function of x of MHD variables, that is, the x component of the electric field E_x, the plasma β, the density ρ, the temperature T, the x and y components of the velocity v_x and v_y, the z, y, and x components of the magnetic field B_z, B_y, and B_x, the intensity of magnetic field $|B|$, and the pressure p from top at $y = 15.7$ (left panel) and at $y = 22.0$ (right panel) for the case of $M_A = 5.0$, $M_S = 1.0$, and $2k_y a = 0.4$ (case D in Figure 2) at $T = 60$. The dashed lines in these panels show initial profiles of those MHD variables; all variables are so normalized that only relative scales are meaningful. In the left panel, MP represents the magnetopause current layer, where B_z has a large gradient. A hatched region designated as VBL is a velocity boundary layer formed just inside the magnetopause current layer. In this layer the flow velocity v_y becomes substantially nonzero, and formation of this velocity boundary layer within the magnetopause current layer is due to the anomalous momentum transport from the magnetosheath into the magnetosphere (onto the closed magnetospheric field lines) by the K-H instability. The right panel shows a cross section passing through the plasma blob; in this case there are three magnetopause current layers. As has been already noted in Figure 3, a quite interesting result seen in this cross section is that in the magnetosphere at $x = -4a \sim 0$ the flow is accelerated substantially (hatched region in v_y profile), and the flow velocity in the y direction v_y reaches almost $2V_0$. This acceleration occurs in coincidence with the increase of E_x in the magnetosphere, where the magnetic field B_z is large, and is hence due to the increase of the $\mathbf{E} \times \mathbf{B}$ flow velocity. For a uniform plasma, such a flow acceleration by the K-H instability leads to a formation of a fast shock discontinuity from an initially subfast shear flow [*Miura*, 1984].

Figure 9 shows profiles in the x direction of spatial averages over one wave period of Reynolds stress (solid lines), Maxwell stress (dashed lines), the x component of the electric field E_x, the plasma momentum in the y direction ρv_y, and the y component of the flow velocity v_y from top for $M_A = 5.0$, $M_S = 1.0$, and $2\ k_y a = 0.8$ (left) and for $M_A = 5.0$, $M_S = 1.0$, and $2k_y a = 0.4$ (right) at their quasi-stationary stages. The stress is normalized by $\rho_0 V_0^2$, and other variables are so normalized that only relative scales are meaningful. The dashed lines in the profile of E_x, ρv_y, and v_y show initial profiles of those MHD variables. For both cases, the Reynolds stress becomes larger than 2% of the flow momentum flux $\rho_0 V_0^2$, and the plasma momentum ρv_y in the magnetosheath is diffused from the magnetosheath into the magnetosphere (hatched region). In coincidence with this momentum transport the magnitude of the electric field $|E_x|$ increases from dashed lines to solid lines.

Notice that those stresses become large where the electric field E_x is amplified. For both cases, the Reynolds stress (solid line) is larger than the Maxwell stress (dashed line). The Reynolds stress for $2k_y a = 0.4$ (right panel) becomes nonzero in much wider region than the case of $2k_y a = 0.8$ (left panel), and the velocity boundary layer for $2k_y a = 0.4$ (right panel) becomes wider than the case of $2k_y a = 0.8$ (left panel). It seems therefore that a longer-wavelength mode leads to a wider velocity boundary layer. In order to evaluate the contribution of the K-H instability to the magnetospheric convection we have calculated the spatial average over one wave period of the convection potential drop (not necessarily electrostatic potential but integral of the electric field) across the boundary layer defined by $\int \langle E_x \rangle\, dx$, where the angular bracket denotes spatial average over one wave period. The ratio of this integral of the electric field to its initial value has been calculated for two

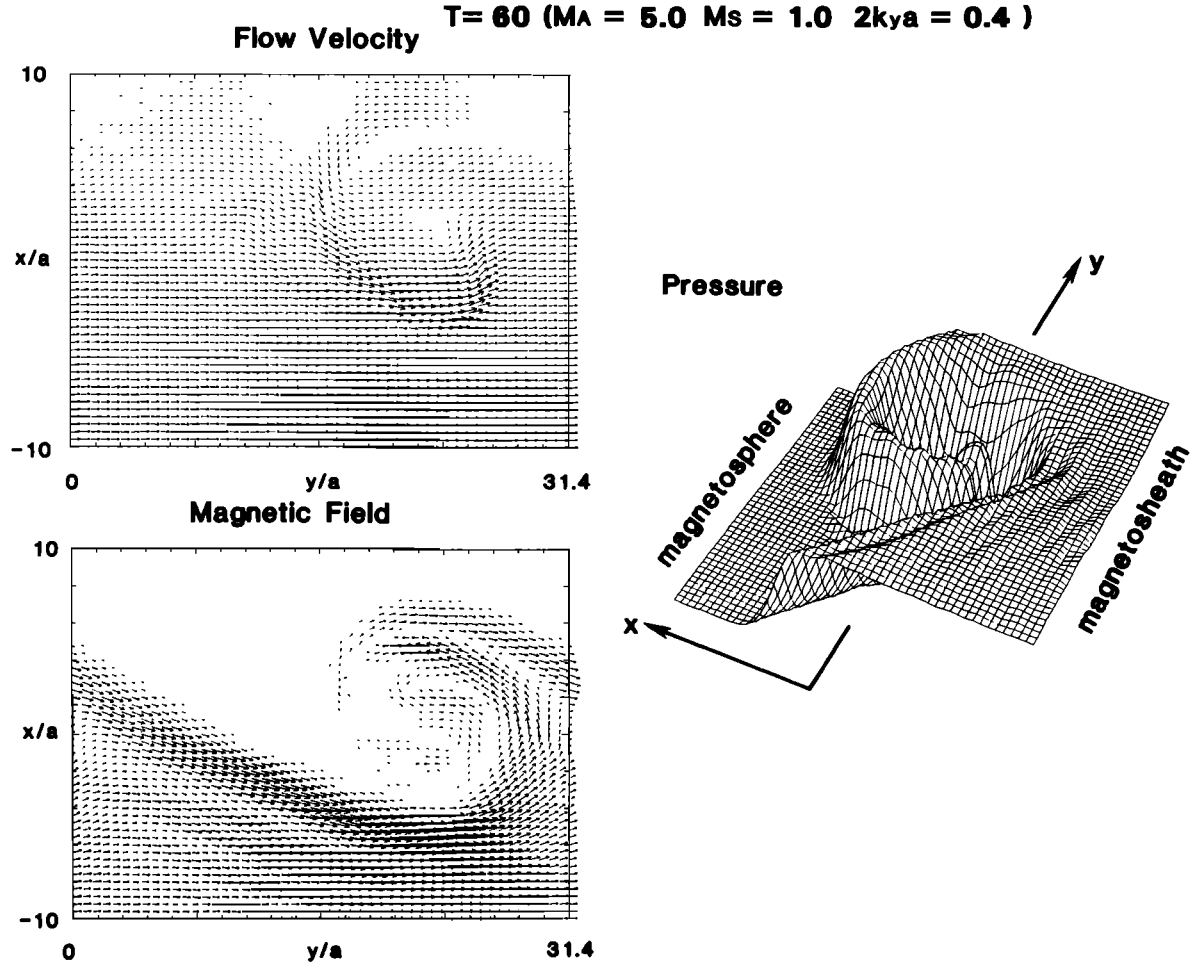

Fig. 7. Flow velocity vectors (top left), magnetic field vectors (bottom left), and three-dimensional view of top surface of the plasma pressure (right) at $T = 60$ for $2k_y a = 0.4$, $M_A = 5.0$, and $M_S = 1.0$ (case D of Figure 2).

different cases shown in Figure 9, and we obtained those ratios of 4.70 (left panel) and 6.46 (right panel); thus the antisunward convection voltage drop (strength) is amplified several times by the anomalous momentum transport associated with the K-H instability, and this ratio is larger for a longer-wavelength mode.

In order to see the dependence of the anomalous momentum transport on the magnetosheath Alfvén Mach number M_A we define the anomalous viscosity according to the definition of eddy viscosity in ordinary hydrodynamics [e.g., *Lamb*, 1945] as follows:

$$\nu_{ano} = -\langle \rho v_x v_y - B_x B_y/\mu_0 \rangle (d\langle \rho v_y \rangle/dx)^{-1}$$

where the bracket represents spatial average over one wave period. The part of ν_{ano} owing to the Reynolds stress $-\rho v_x v_y$ is the anomalous eddy viscosity in ordinary hydrodynamics, and the part due to the Maxwell (magnetic) stress $B_x B_y/\mu_0$ is the anomalous magnetic viscosity [e.g., *Eardley and Lightman*, 1975]. Figure 10 shows time evolutions of the eddy viscosity ν_{eddy}, the magnetic viscosity ν_{mag}, and the total (eddy plus magnetic) anomalous viscosity ν_{ano} normalized by $2aV_0$ at $x = 0$ for $M_A = 5$ and $2k_y a = 0.8$ (case B in Figure 2). All viscosities grow exponentially with time, reach the maximum values at $T = 36 \sim 38$, and then decay. At $T = 37$ the anomalous viscosity becomes $\sim 0.2 \times 2aV_0$. Figure 11 shows the dependence of the maximum anomalous viscosity at $x = 0$ attained during the time evolution on the Alfvén Mach number M_A in the magnetosheath. For $M_A = 2.5$ the anomalous viscosity ν_{ano} is minimum and equal to $\sim 0.014 \times 2aV_0$, and with the increase of M_A from 2.5 to 6.0 the anomalous viscosity ν_{ano} increases, and for M_A larger than 5.0 it reaches almost constant value $\sim 0.2 \times 2aV_0$. Therefore depending on the value of the Alfvén Mach number M_A in the magnetosheath, the anomalous viscosity ν_{ano} takes a value of $0.01\text{–}0.2 \times 2aV_0$. Figure 12 shows the ratio of the magnetic viscosity ν_{mag} at $x = 0$ to the eddy viscosity ν_{eddy} at $x = 0$ as a function of M_A. For $M_A = 2.5$, ν_{mag} is comparable to ν_{eddy}, but this ratio decreases considerably with the increase of M_A.

4. SUMMARY AND DISCUSSION

For a realistic model of the dayside low-latitude magnetospheric boundary characterized by gradients of plasma and magnetic field normal to the magnetopause we have performed MHD simulations of Kelvin-Helmholtz instability. Important results obtained by these simulations are summarized as follows:

1. The magnetopause current layer is highly nonlinearly corrugated by the K-H instability, and a plasma blob is

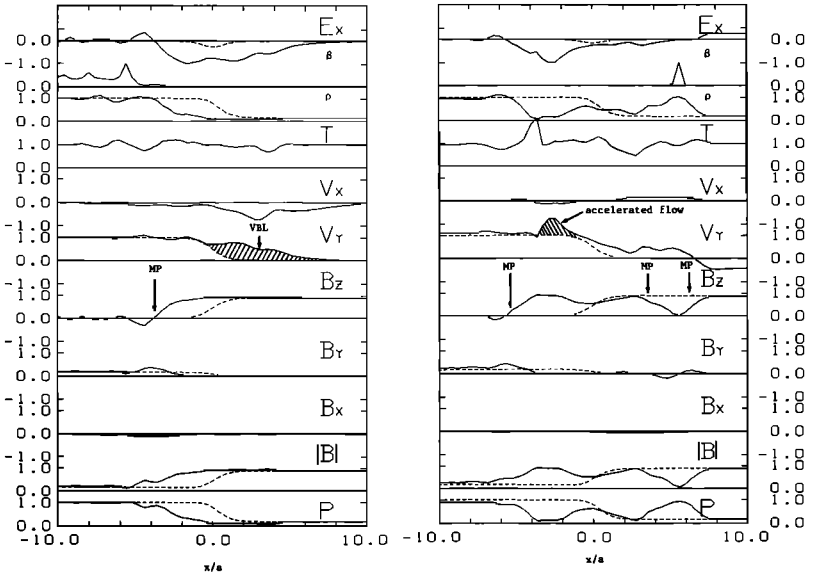

Fig. 8. Profiles as a function of x of MHD variables, that is, the x component of the electric field E_x; the plasma β; the density ρ; the temperature T; the x and y components of the velocity v_x and v_y; the z, y, and x components of the magnetic field B_z, B_y, and B_x; the intensity of magnetic field $|B|$; and the pressure p from top at $y = 15.7$ (left panel) and at $y = 22.0$ (right panel) for the case of $M_A = 5.0$, $M_S = 1.0$, and $2k_y a = 0.4$ (case D in Figure 2) at $T = 60$. The dashed lines in these panels show initial profiles of those MHD variables. MP is the magnetopause current layer, and VBL is a velocity boundary layer formed just inside the magnetopause current layer.

formed by the interchange motion associated with the K-H instability.

2. The corrugation of the magnetopause current layer becomes more noticeable with the increase of the magnetosheath Alfvén Mach number M_A, where M_A is defined by using a magnetosheath magnetic field component parallel to the magnetosheath flow.

3. A wide velocity boundary layer is formed just inside the magnetopause current layer by the anomalous momentum transport associated with the K-H instability.

4. Where the vortex motion is added onto the undisturbed background flow, the plasma flow is accelerated substantially by the K-H instability. This flow acceleration is due to the increase in the electric field drift $\mathbf{E} \times \mathbf{B}$.

5. For a longer-wavelength mode the saturation amplitude of the K-H instability becomes larger, and the corrugation of the magnetopause current layer occurs in much wider region in the x direction.

6. The convection electric field in the magnetosphere responsible for the $\mathbf{E} \times \mathbf{B}$ sheared plasma flow is amplified by the K-H instability, and the total voltage drop (not necessarily electrostatic potential but an integral of the electric field) across the velocity boundary layer is amplified several times.

7. The magnetosheath plasma flow momentum is diffused into the magnetosphere by the anomalous tangential (Reynolds plus Maxwell) stresses associated with the K-H instability, and the velocity shear layer is widened by the instability, whereas the thickness of the magnetopause current

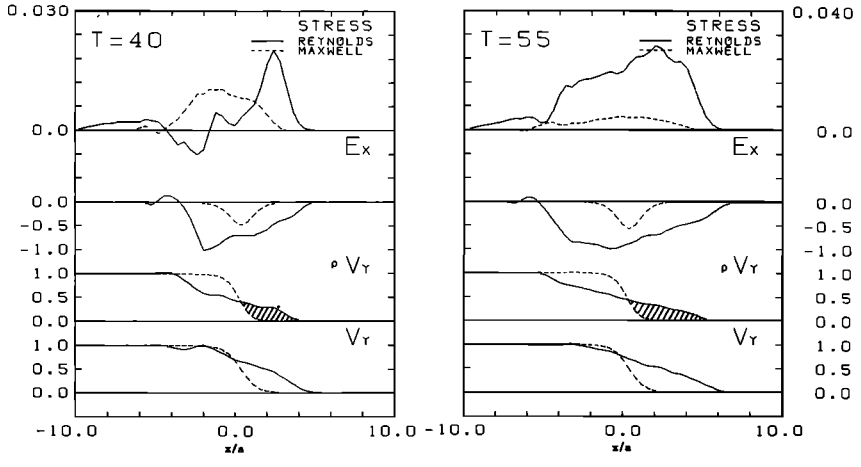

Fig. 9. Profiles in the x direction of spatial average over one wave period of Reynolds stress (solid lines), Maxwell stress (dashed lines), the x component of the electric field E_x, the plasma momentum in the y direction ρv_y, and the y component of the flow velocity v_y from top for $M_A = 5.0$, $M_S = 1.0$, and $2k_y a = 0.8$ (left panel) and for $M_A = 5.0$, $M_S = 1.0$, and $2k_y a = 0.4$ (right panel) at their quasi-stationary stages.

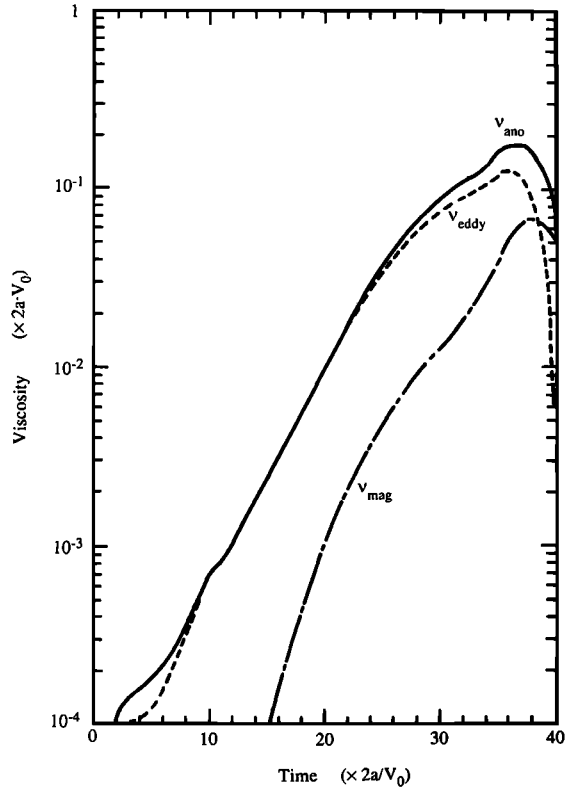

Fig. 10. Time evolutions of the eddy viscosity ν_{eddy}, the magnetic viscosity ν_{mag}, and the total (eddy plus magnetic) anomalous viscosity ν_{ano} at $x = 0$ for $M_A = 5$ and $2k_y a = 0.8$ (case B in Figure 2).

layer remains almost constant. The total stress reaches 0.6 to a few percent of the magnetosheath flow momentum flux.

8. The value of the anomalous viscosity ν_{ano} depends importantly on the magnetosheath Alfvén Mach number M_A defined by the magnetosheath magnetic field component parallel to the magnetosheath flow velocity. For $M_A = 2.5$, ν_{ano} is equal to $\sim 0.014 \times 2aV_0$ and it increases with M_A, and for $M_A > 5.0$ it is equal to $\sim 0.2 \times 2aV_0$.

The present simulation results indicate that the magnetopause current layer is highly nonlinearly corrugated by the K-H instability. These results are consistent with observations by *Aubry et al.* [1971] of large-amplitude oscillations of magnetopause. According to *Aubry et al.* [1971], the large-amplitude oscillations of the magnetopause have periods from 3.5 to 6 min. For the fastest growing unstable mode treated in the present simulation we have $2ak_y = 0.8$ and $\omega_r/k_y = V_0/2$. Therefore if we assume $a = 1000$–3000 km and $V_0 = 300$ km/s, we obtain the wavelength of the fastest growing mode of the K-H instability $\lambda = 16 \times 10^3$–47×10^3 km, and its wave period $\tau = 107$–313 s, which is comparable to the observed periods of the boundary oscillations. The formation of a wide velocity boundary layer within the magnetopause current layer (see left panel of Figure 8) as a result of the K-H instability is consistent with observations of a tailward flow in the low-latitude boundary layer by *Eastman and Hones* [1979] and *Williams et al.* [1985]. Furthermore, the present results showing that a plasma blob is formed by the K-H instability and that the velocity boundary layer has a variable thickness and contains plasma eddies are in reasonable agreement with observations by *Sckopke et al.* [1981] if we interpret that in their observation a satellite is passing through the plasma blob formed by the K-H instability.

In the present two-dimensional model of the K-H instability at the magnetospheric boundary we have neglected a fact that magnetic field lines in the magnetosphere are tied to the ionosphere. We have also assumed in the present model that the magnetosheath flow velocity is smaller than twice the fast magnetosonic speed, although actually the magnetosheath flow velocity reaches twice the fast magnetosonic speed at somewhere in downstream flank. For superfast shear flow with $V_0/v_f > 2$, where v_f is the fast magnetosonic speed, the evanescent eigenmode is no more unstable, and the K-H instability becomes unstable only when the radiating boundary condition is imposed [*Blumen et al.*, 1977; *Drazin and Davey*, 1977]. The energy being radiated from such a superfast shear layer, the growth rate of the K-H instability for the superfast shear flow in the downstream flank, is quite small compared with the growth rate for the subfast shear flow on the dayside; therefore although we may consider that the K-H instability is dynamically important as a viscouslike drag where the magnetosheath flow speed remains smaller than twice the fast magnetosonic speed, the consequence of the K-H instability in the downstream flank, where the velocity jump becomes larger than twice the fast magnetosonic speed, is not obvious from the present simulation.

From above considerations it is apparent that in considering K-H instability at the magnetopause we must notice the presence of two important time scales τ_w and τ_d, where τ_w is a travel time of the Alfvén wave propagating from the magnetopause to the ionosphere and returning back to the magnetopause after reflection from the ionosphere and τ_d is a dynamical time scale required for the magnetosheath flow to

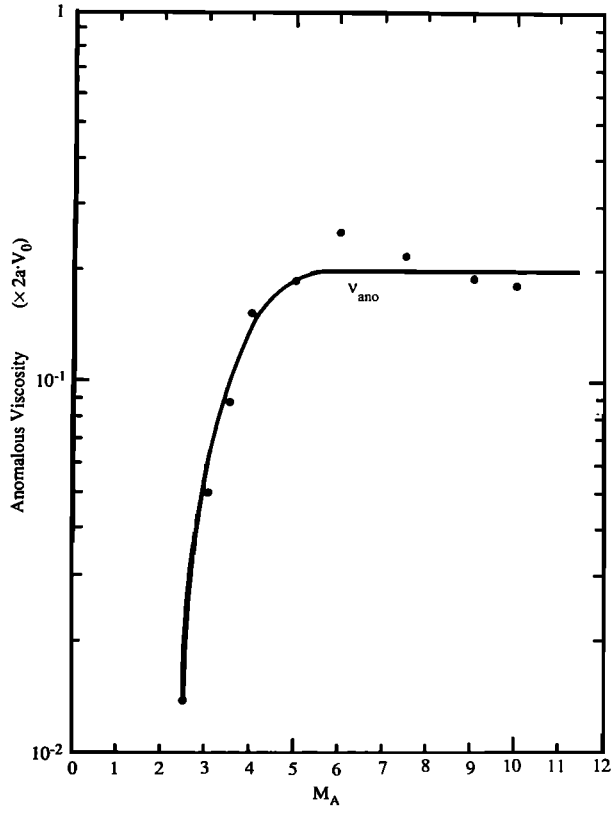

Fig. 11. The dependence of the maximum anomalous viscosity at $x = 0$ attained during the time evolution on the magnetosheath Alfvén Mach number M_A.

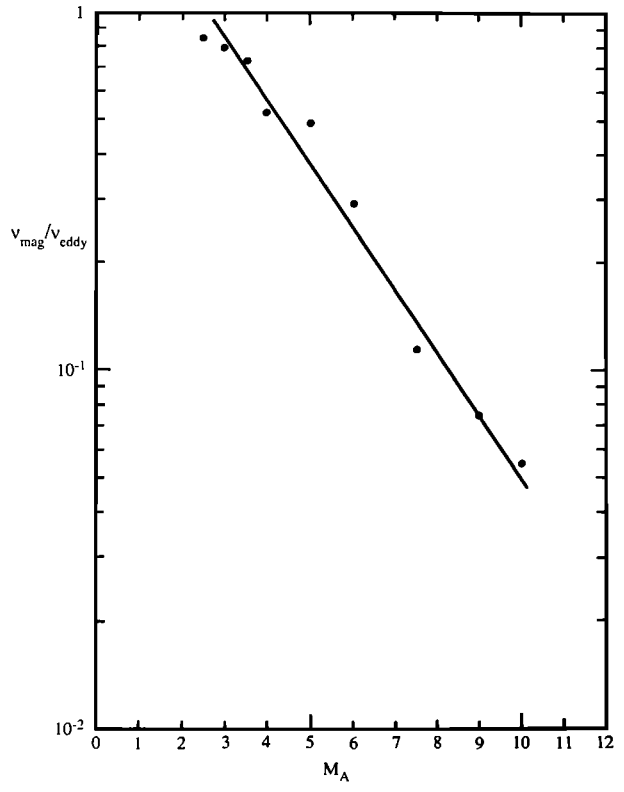

Fig. 12. The ratio of the magnetic viscosity ν_{mag} at $x = 0$ to the eddy viscosity ν_{eddy} at $x = 0$ as a function of M_A.

travel from the subsolar point to a point, where $V_0/v_f = 2$ is satisfied on the downstream flank of the magnetosphere.

For the fastest growing mode of the K-H instability we obtain

$$\gamma_{KH}\tau_w \sim 0.2(V_0/v_A)(l_{||}/2a)$$

where γ_{KH} is the growth rate of the K-H instability, V_0 is the total jump of the flow velocity across the boundary, v_A is the average Alfvén speed along closed field lines inside the boundary, $l_{||}$ is the length of the closed field line, and $2a$ is the thickness of the velocity shear layer. For a reasonable set of parameters at the dayside magnetopause, that is, $V_0 = 200$ km/s, $v_A = 2000$ km/s, $l_{||} = 20\ R_E$, and $2a = 1000$ km [*Berchem and Russell*, 1982] we obtain $\gamma_{KH}\tau_w \sim 3$. It is therefore reasonable to assume that although the growth rate of the K-H instability may be reduced somewhat by the three-dimensional effect by coupling to the ionosphere, the stability of the magnetopause boundary itself is not altered by this three-dimensional effect; namely, the K-H instability at the magnetopause boundary cannot be suppressed by this three-dimensional effect.

For a reasonable set of parameters we also obtain $\gamma_{KH}\tau_d \sim l_d/\lambda \sim l_d/l_e \sim 4$, where l_e is the e-folding distance of the fastest growing mode of the K-H instability, λ is the wavelength of that mode, and l_d is the distance from the subsolar point to the point where $V_0/v_f \sim 2$ is satisfied (in the absence of knowledge on where $V_0/v_f \sim 2$ is satisfied we have assumed that l_d is comparable to the distance from the subsolar point to dawn or dusk flank of the magnetosphere); therefore the K-H instability can e-fold several times and can impose a substantial tangential stress on the boundary before the magnetosheath flow reaches a tail flank. In a highly nonlinear stage of the K-H instability the longest possible wavelength mode of the K-H instability may dominate the plasma dynamics (*Pritchett and Coroniti* [1984]; a similar tendency that a wavelength of the instability increases with a spatial growth of the instability is also seen in *Wu*'s [1986] simulation of the convective K-H instability); however, in view of the fact that the dynamical time scale τ_d over the dayside magnetopause is finite and not much larger than the e-folding time of the K-H instability, only the K-H mode which has a linear growth rate comparable to that of the linearly fastest growing mode of the K-H instability is expected to have enough time to grow into a large amplitude and to have a dominant effect in imposing the tangential stress on the flank side of the magnetospheric boundary. Such a speculation is consistent with the fact that the observed wavelength of the boundary wave (ripple) on the dayside magnetopause boundary [*Lepping and Burlaga*, 1979] is 47×10^3 km and is comparable to the wavelength of the linearly fastest growing mode of the K-H instability.

It should be emphasized here that although a saturation of the K-H instability in the present simulation occurs under the use of the idealized boundary condition, that is, the periodic boundary condition in the y direction, the saturation mechanism in the present simulation is essentially a nonlinear process as in the case of the actual K-H instability at the magnetopause; namely, the saturation of the K-H instability occurs by the anomalous momentum transport from magnetosheath into the magnetosphere by the finite Reynolds stress $-\rho v_x v_y$ and Maxwell stress $B_x B_y/\mu_0$, which relax the velocity shear profile. In the present simulation an initial seed of the unstable perturbation is chosen to have a wavelength equal to the periodicity length. Therefore the role of the boundary condition in the y direction, that is, to impose a periodic boundary condition at boundaries, is just to select a mode which has a wavelength equal to the periodicity length. In simulation runs A, B, and C this periodicity length is equal to the wavelength of a linearly fastest growing mode of the K-H instability. Since the linearly fastest growing mode is a mode, which grows fastest, this mode dominates the plasma dynamics in the early phase of the K-H instability, and it imposes a finite tangential stress on the magnetopause boundary. Therefore when the dynamical time scale τ_d is finite and not much larger than the e-folding time of the fastest growing mode of the K-H instability, this linearly fastest growing mode plays a dominant role in imposing the finite tangential stress on the magnetopause boundary. On the opposite situation, when the dynamical time scale τ_d is much larger than the e-folding time of the fastest growing mode of the K-H instability, we expect that the longest possible wavelength mode has enough time to grow into a large amplitude and is therefore responsible for imposing a finite tangential stress on the magnetopause boundary; as we have seen, however, at the dayside magnetopause, τ_d seems to be rather small if l_d is really comparable to the distance from the subsolar point to dawn or dusk flank of the magnetosphere. Therefore on the basis of an assumption that τ_d for the terrestrial magnetosphere is not much larger than the e-folding time of the fastest growing mode of the K-H instability, we may be able to justify to use the periodic condition with the periodicity length equal to the wavelength of the fastest growing mode for evaluating the nonlinear tangential stress by the K-H instability at the magnetopause.

Although the K-H instability in the magnetospheric inertial frame is likely to be convective (that is, growing spatially with

distance), the instability becomes absolute in the wave frame moving with a speed $V_0/2$ (notice that the wave dispersion of the K-H instability in the magnetospheric inertial frame is $\omega_r/k_y = V_0/2$). Therefore the difference between the absolute growth and the convective growth does not seem to be essential for considering the effect of the K-H instability on the momentum transport at the magnetopause. Instead, the most essential point in considering the effect of the K-H instability on the momentum transport seems to be determining a wavelength of the K-H instability which dominates the plasma dynamics at the magnetopause, since the saturation amplitude of that mode and hence the anomalous momentum flux by that mode depends on the wavelength of the K-H mode as we have seen in Figure 2 (that is, a longer-wavelength mode has a larger saturation amplitude and a larger stress; see also *Pritchett and Coroniti* [1984]). *Wu* [1986] has made an MHD simulation of the K-H instability for convective case, where the setup of the simulation and the boundary condition are so chosen that the wavelength of the K-H instability is allowed to change in the evolution of the K-H instability. As was pointed out already, the observation of boundary wave on the dayside magnetopause [*Lepping and Burlaga*, 1979] seems to suggest that the wavelength of the most dominant mode of the K-H instability at the magnetopause is close to the wavelength of the fastest growing unstable mode of the K-H instability. On the basis of these discussions we use in the following the result of the evaluation of the anomalous momentum transport in section 3 for evaluating the anomalous momentum transport by the K-H instability in the solar wind–magnetosphere interaction.

Here we should mention the role of the initial seed of the K-H instability. In the present simulation we initiate the simulation by adding an initial seed of unstable perturbation with a peak velocity v_x equal to $0.005V_0$ to the flowing equilibrium. Such a seed perturbation is also necessary for the actual K-H instability at the magnetopause. Since the magnetosheath flow in the downstream of the bow shock includes many kinds of perturbations, we expect that those finite amplitude perturbations play a role of the initial seed for the K-H instability. Although the amplitude of such a perturbation is unknown, the fact that the magnetopause is nearly always in motion [e.g., *Williams*, 1980] possibly by the K-H instability suggests that the perturbation (seed) of sufficient amplitude (sufficient so that the K-H unstable mode saturates after several *e*-folding growths of the mode) is nearly always present at the subsolar region of the magnetopause, where the K-H instability is initiated.

Regarding the anomalous momentum transport by the K-H instability, the present simulation results indicate that the anomalous viscosity by the K-H instability ν_{ano} reaches ~ 0.01–$0.2 \times 2aV_0$, and the anomalous stress (anomalous momentum flux) reaches ~ 0.006–$0.03 \times \rho_0 V_0^2$, where V_0 is the total velocity jump and $2a$ is the thickness of the velocity shear layer. If we substitute a reasonable set of parameters on the dayside magnetopause, $2a \sim 1000$ km [*Berchem and Russell*, 1982], $V_0 \sim 100$ km/s, into the above viscosity formula we obtain $\nu_{ano} \sim 10^{13}$–2×10^{14} cm^2/s. This value of the anomalous viscosity, which is comparable to the Bohm diffusion rate at the magnetopause [*Miura*, 1984], is just the right magnitude for driving a magnetospheric convection (plasma circulation) in the terrestrial magnetosphere [*Axford and Hines*, 1961; *Hill*, 1979]; in this context it is interesting to note that *Paschmann et al.* [1985] have found that a substantial dissipation, which is viscous in nature, is present in a rotational discontinuity and that viscosity is comparable to the Bohm diffusion rate. Although the present simulation of the K-H instability is performed for the tangential discontinuity, there is no reason why the K-H instability does not occur in the rotational discontinuity if there is a velocity shear in the rotational discontinuity. As we have seen, the K-H instability seems to provide a fundamental mechanism yielding required anomalous (eddy plus magnetic) viscosity for the "viscouslike interaction" hypothesis [*Axford and Hines*, 1961], which could explain an observed residual magnetospheric plasma convection (circulation) not controlled by the north-south component of the interplanetary magnetic field [*Reiff et al.*, 1981; *Wygant et al.*, 1983; *Doyle and Burke*, 1983] (see also a review by *Cowley* [1982]). According to *Hill* [1979], the total number of solar wind ions per second traversing the cross-sectional area of earth's magnetosphere is $\sim 1.6 \times 10^{29}$ s^{-1}. On the other hand, the particle flux of ions in the low-latitude boundary layer which is transported tailward into the magnetotail is 2–10×10^{26} s^{-1} [*Eastman*, 1984]. Therefore the particle flux that is necessary for constituting the low-latitude boundary layer is 0.1–0.6% of the total incident solar wind number flux. If we assume the momentum flux is just equal to the number flux multiplied by the proton mass and solar wind speed, the necessary momentum flux that constitutes the low-latitude boundary layer is 0.1–0.6% of the total incident solar wind momentum flux. As we have seen, this momentum flux is sufficiently provided by the anomalous momentum flux of the K-H instability, which reaches 0.6–3.0% of the incident solar wind momentum flux.

We have seen in Figure 9 that the initial convection voltage drop is amplified more than 5 times by the K-H instability. Without instabilities the voltage drop across the magnetopause is of the order of the typical ion thermal energy divided by the electronic charge. Therefore if we assume that there is a voltage drop of ~ 1kV across the magnetospheric boundary near the subsolar region, where the K-H instability is initiated, assuming the abundance of ~ 1 keV protons, this voltage drop (not necessarily electrostatic potential difference but the integral of the electric field) is amplified about 5 times by the K-H instability; therefore the total voltage drop including dawn and dusk contributions becomes ~ 10 kV. This value of the convection voltage drop by the K-H viscouslike interaction, when mapped over the polar cap, is consistent with observed value (5–30 kV) of the residual component of the magnetospheric convection which is not controlled by the north-south component of the interplanetary magnetic field [*Reiff et al.*, 1981; *Wygant et al.*, 1983; *Doyle and Burke*, 1983] (see also *Williams et al.* [1985] and *Baumjohann and Haerendel* [1985]). A more direct search for evidence on viscouslike interaction at the dusk magnetopause by *Mozer* [1984] shows that the voltage drop across the dusk magnetopause is at times extremely small (<1 kV), and hence the viscouslike interaction is negligibly small at those times. According to the present picture of the K-H viscouslike interaction, such an observation may be explained by a speculation that at those times the magnetosheath flow velocity remains sub-Alfvénic with respect to the magnetosheath magnetic field component parallel to the flow velocity, and thus the K-H instability is suppressed by the large magnetic tension force.

By using a model of the magnetospheric boundary including gradients of plasma and magnetic field normal to the magnetopause it has been demonstrated that a dayside low-

latitude magnetospheric boundary is a highly dynamic boundary under the presence of the K-H instability. The wavelength and the wave period of the K-H instability are in good agreement with observations of boundary oscillations at the magnetopause. A wide velocity boundary layer is formed just inside the magnetopause current layer by the anomalous momentum transport (anomalous viscosity) associated with the K-H instability, and the anomalous momentum flux into the magnetosphere is sufficient for accounting for the observed tailward momentum flux in the low-latitude boundary layer. The anomalous viscosity obtained is just the right magnitude for driving a magnetospheric convection in the terrestrial magnetosphere and the magnitude of the anomalous viscosity depends importantly on the magnetosheath Alfvén Mach number, which is defined by using the magnetosheath magnetic field component parallel to the magnetosheath flow velocity.

Acknowledgments. This work was supported, in part, by Grants-in-Aid for Scientific Research, 59740203, provided by the Japanese Ministry of Education, Science and Culture.

The Editor thanks W. J. Keikkila and C. C. Wu for their assistance in evaluating this paper.

REFERENCES

Aubry, M. P., M. G. Kivelson, and C. T. Russell, Motion and structure of the magnetopause, *J. Geophys. Res.*, *76*, 1673, 1971.

Axford, W. I., and C. O. Hines, A unifying theory of high-latitude geophysical phenomena and geomagnetic storms, *Can. J. Phys.*, *39*, 1433, 1961.

Baumjohann, W., and G. Haerendel, Magnetospheric convection observed between 0600 and 2100 LT: Solar wind and IMF dependence, *J. Geophys. Res.*, *90*, 6370, 1985.

Berchem, J., and C. T. Russell, The thickness of the magnetopause current layer ISEE 1 and 2 observations, *J. Geophys. Res.*, *87*, 2108, 1982.

Blumen, W., P. G. Drazin, and D. F. Billings, Shear layer instability of an inviscid compressible fluid, 3, *J. Fluid Mech.*, *82*, 255, 1977.

Cowley, S. W. H., The causes of convection in the earth's magnetosphere: A review of developments during the IMS, *Rev. Geophys.*, *20*, 531, 1982.

Doyle, M. A., and W. J. Burke, S3-2 measurements of the polar cap potential, *J. Geophys. Res.*, *88*, 9125, 1983.

Drazin, P. G., and A. Davey, Shear layer instability of a compressible fluid, 3, *J. Fluid Mech.*, *82*, 255, 1977.

Dungey, J. W., Electrodynamics of the outer atmosphere, in *Proceedings of the Ionosphere*, p. 255, Physical Society of London, 1955.

Dungey, J. W., Interplanetary magnetic field and the auroral zones, *Phys. Rev. Lett.*, *6*, 47, 1961.

Eardley, D. M., and A. P. Lightman, Magnetic viscosity in relativistic accretion disks, *Astrophys. J.*, *200*, 187, 1975.

Eastman, T. E., Observations of the magnetospheric boundary layers, Proceedings of the Conference on Achievements of the International Magnetospheric Study, *ESA SP-217*, Eur. Space Agency, Graz, Austria, 1984.

Eastman, T. E., and E. W. Hones, Jr., Characteristics of the magnetospheric boundary layer and magnetopause layer as observed by IMP 6, *J. Geophys. Res.*, *84*, 2019, 1979.

Gerwin, R. A., Stability of the interface between two fluids in relative motion, *Rev. Mod. Phys.*, *40*, 652, 1968.

Hill, T. W., Rates of mass, momentum, and energy transfer at the magnetopause, in Proceedings of Magnetospheric Boundary Layers Conference, *Eur. Space Agency Spec. Publ., ESA SP 148*, 325, 1979.

Lamb, S. H., *Hydrodynamics*, 6th ed., Cambridge University Press, New York, 1945.

Lapidus, A., A detached shock calculation by second-order finite differences, *J. Comput. Phys.*, *2*, 154, 1967.

Lepping, R. P., and L. F. Burlaga, Geomagnetopause surface fluctuations observed by Voyager 1, *J. Geophys. Res.*, *84*, 7099, 1979.

Levy, R. H., H. E. Petschek, and G. L. Siscoe, Aerodynamic aspects of the magnetospheric flow, *A.I.A.A.J.*, *2*, 2065, 1964.

Miura, A., Nonlinear evolution of the magnetohydrodynamic Kelvin-Helmholtz instability, *Phys. Rev. Lett.*, *49*, 779, 1982.

Miura, A., Anomalous transport by magnetohydrodynamic Kelvin-Helmholtz instabilities in the solar wind–magnetosphere interaction, *J. Geophys. Res.*, *89*, 801, 1984.

Miura, A., Anomalous transport by Kelvin-Helmholtz instabilities, in *Computer Simulation of Space Plasmas*, edited by H. Matsumoto and T. Sato, pp. 203–224, D. Reidel, Hingham, Mass., 1985*a*.

Miura, A., Kelvin-Helmholtz instability at the magnetospheric boundary, *Geophys. Res. Lett.*, *12*, 635, 1985*b*.

Mozer, F. S., Electric field evidence on the viscous interaction at the magnetopause, *Geophys. Res. Lett.*, *11*, 135, 1984.

Papamastorakis, I., G. Paschmann, N. Sckopke, S. J. Bame, and J. Berchem, The magnetopause as a tangential discontinuity for large rotation angles, *J. Geophys. Res.*, *89*, 127, 1984.

Parker, E. N., Dynamics of the interplanetary gas and magnetic fields, *Astrophys. J.*, *128*, 6640, 1958.

Parker, E. N., Confinement of a magnetic field by a beam of ions, *J. Geophys. Res.*, *72*, 2315, 1967.

Paschmann, G., I. Papamastorakis, N. Sckopke, B. U. O. Sonnerup, S. J. Bame, and C. T. Russell, ISEE observations of the magnetopause: Reconnection and the energy balance, *J. Geophys. Res.*, *90*, 12,111, 1985.

Petschek, H. E., Magnetic field annihilation, *NASA Spec. Publ. SP-50*, 425, 1964.

Pritchett, P. L., and F. V. Coroniti, The collisionless macroscopic Kelvin-Helmholtz instability, 1, Transverse electrostatic mode, *J. Geophys. Res.*, *89*, 168, 1984.

Reiff, P. H., R. W. Spiro, and T. W. Hill, Dependence of polar cap potential drop on interplanetary parameters, *J. Geophys. Res.*, *86*, 7639, 1981.

Richtmyer, R. D., and K. W. Morton, *Difference methods for initial value problems*, 2nd ed., Wiley-Interscience, New York, 1967.

Sckopke, N., G. Paschmann, G. Haerendel, B. U. O. Sonnerup, S. J. Bame, T. G. Forbes, E. W. Hones, Jr., and C. T. Russell, Structure of the low-latitude boundary layer, *J. Geophys. Res.*, *86*, 2099, 1981.

Sonnerup, B. U. O., Magnetic field reconnection, in *Solar System Plasma Physics*, vol. 3, edited by L. J. Lanzerotti, C. F. Kennel, and E. N. Parker, p. 94, North-Holland, Amsterdam, 1979.

Southwood, D. J., Magnetopause Kelvin-Helmholtz instability, in Proceedings of magnetospheric boundary layers conference, *Eur. Space Agency Spec. Publ., ESA SP 148*, 357, 1979.

Vasyliunas, V. M., Theoretical models of magnetic field line merging, 1, *Rev. Geophys.*, *13*, 303, 1975.

Williams, D. J., Magnetopause characteristics at 0840–1040 hours local time, *J. Geophys. Res.*, *85*, 3387, 1980.

Williams, D. J., D. G. Mitchell, T. E. Eastman, and L. A. Frank, Energetic particle observations in the low-latitude boundary layer, *J. Geophys. Res.*, *90*, 5097, 1985.

Wu, C. C., Kelvin-Helmholtz instability at the magnetopause boundary, *J. Geophys. Res.*, *91*, 3042, 1986.

Wygant, J. R., R. B. Torbert, and F. S. Mozer, Comparison of S3-3 polar cap potential drops with the interplanetary magnetic field and models of magnetopause reconnection, *J. Geophys. Res.*, *88*, 5727, 1983.

A. Miura, Geophysics Research Laboratory, Faculty of Science, University of Tokyo, Bunkyo-ku, Tokyo 113, Japan.

(Received June 20, 1986;
revised December 10, 1986;
accepted December 29, 1986.)